Search for More Stable $C_{58}X_{18}$ Isomers: Stabilities and Electronic Properties of Seven-Membered Ring $C_{58}X_{18}$ Fullerene Derivatives (X = H, F, and Cl)

De-Li Chen,[†] Wei Quan Tian,*[,†] Ji-Kang Feng,[†,‡] and Chia-Chung Sun[†]

State Key Laboratory of Theoretical and Computational Chemistry, Institute of Theoretical Chemistry, Jilin University, Changchun 130023, China, and College of Chemistry, Jilin University, Changchun 130023, China

Received: January 16, 2007; In Final Form: March 23, 2007

Stimulated by recent preparation and characterization of the first $C_{58}F_{18}$ fullerene derivative, with a heptagon in the framework (Science, **2005**, *309*, 278), we have performed systematic density functional studies on the stabilities and electronic properties of two different structures $C_{58}X_{18}$ (**A**) and $C_{58}X_{18}$ (**B**), where X = H, F, and Cl. The large energy gaps between the highest occupied molecular orbitals and the lowest unoccupied molecular orbitals (between 2.64 and 3.45 eV) and the aromatic character (with nucleus independent chemical shifts from −10.0 to −13.9 ppm) of $C_{58}X_{18}$ (**A**) and $C_{58}X_{18}$ (**B**) indicate that they possess high stabilities. Further investigations show that the heats of formation of $C_{58}X_{18}$ fullerene derivatives are highly exothermic, suggesting that adding nine X_2's releases much of the strain of pure C_{58} fullerene and leads to stabilities of the derivatives. Lower in energy and stronger in aromatic character than $C_{58}F_{18}$ (**B**), which has been experimentally characterized, $C_{58}F_{18}$ (**A**) should also be isolated. In addition, $C_{58}F_{18}$ and $C_{58}Cl_{18}$ are predicted to possess large electron affinities, especially for $C_{58}F_{18}$ (**B**) and $C_{58}Cl_{18}$ (**B**) with values of 3.00 and 3.06 eV, respectively, even larger than that (2.50 eV) of $C_{60}F_{18}$. Hence, $C_{58}F_{18}$ and $C_{58}Cl_{18}$ can serve as good electron-acceptors with possible photonic/photovoltaic application. The IR spectra of $C_{58}X_{18}$ are simulated to facilitate identification of different isomers experimentally. In addition, the electronic spectra and second-order hyperpolarizabilities of $C_{58}X_{18}$ are predicted by ZINDO and sum-over-states model. With the addition of $9X_2$, both the static and frequency-dependent second-order hyperopolarizabilities of $C_{58}X_{18}$ greatly decrease compared to those of C_{58}.

I. Introduction

Due to the potential applications[1−5] of fullerenes as new agents and materials for molecular electronics, nanoprobes, superconductors, and nonlinear optics, there has been greatly scientific interest focusing not only on the extent of C_{60}, C_{70}, and some higher fullerenes but also on the fullerenes smaller than C_{60}. Pure carbon cages (fullerenes) characterized so far basically satisfy the isolated pentagon rule (IPR),[6,7] while fullerenes smaller than C_{60} must have strained pentagon−pentagon fusions and show high lability. As a result, bulk synthesis of smaller fullerenes becomes extremely difficult. Recently, Xie's preparation of $C_{50}Cl_{10}$ provides a route to the bulk synthesis of smaller fullerenes and their derivatives and provides new insights into the mechanism of fullerene formation.[8]

The possibility for fullerenes to have heptagon (quasifullerenes) was first proposed in 1992 by Taylor.[9] Calculations suggested that cages with a heptagon fall with in the classical fullerene energy range.[10] In particular, a quasifullerene C_{62} with a heptagon is predicted to have lower energy than all of the 2385 classical fullerene isomers based on the predictions from several different levels of theory,[11] and a heptagonal C_{58} fullerene is calculated to be only 2.50 kcal/mol less stable than the most stable classical fullerene isomer.[12−17] These predictions suggest that some quasifullerenes with a heptagon in their frameworks should also be important components during the generation of fullerenes. However, the capture of the fullerene isomers with heptagons has not been succeeded experimentally. Until very recently,[18] fluorination of C_{60} at 550 °C leads to milligram quantities of two stable fullerene derivatives with 58-carbon cage structure ($C_{58}F_{18}$ and $C_{58}F_{17}CF_3$), and the spectroscopy data support a heptagon in the framework. These observations indicate that C_{58} and its derivatives are interesting systems to be understood and obviously deserve further efforts of detailed theoretical studies to determine their energetics, stabilities, and electronic properties. In this work, systematic investigations on the stabilities, magnetics, and electronic and optical properties of two different structures of $C_{58}X_{18}$ (X = H, F, and Cl) fullerene derivatives are carried out within density functional theory based methods and semiempirical method.

II. Computational Details

The initial geometries of $C_{58}X_{18}$ (X = H, F, and Cl) are optimized with B3LYP/3-21G (ref 19) method, and some of them are refined at B3LYP/6-31G(d,p) level within GAUSSIAN 03 package.[20] All of the electronic properties of the fullerene derivatives considered in our study are analyzed based on the B3LYP/6-31G(d,p) geometries. Besides, aromaticity of fullerene derivatives is evaluated by calculating the nucleus-independent chemical shifts (NICS)[21,22] based on GIAO-B3LYP/6-31G(d,p)//B3LYP/6-31G(d,p) method. The natural bond orbital (NBO)[23,24] analysis is adopted to evaluate the natural atomic charges of the atoms within fullerene derivatives. Electronic spectra and

* Corresponding author. E-mail: tianwq@jlu.edu.cn.
† Institute of Theoretical Chemistry, Jilin University.
‡ College of Chemistry, Jilin University.

10.1021/jp070377s CCC: $37.00
Published on Web 04/26/2007

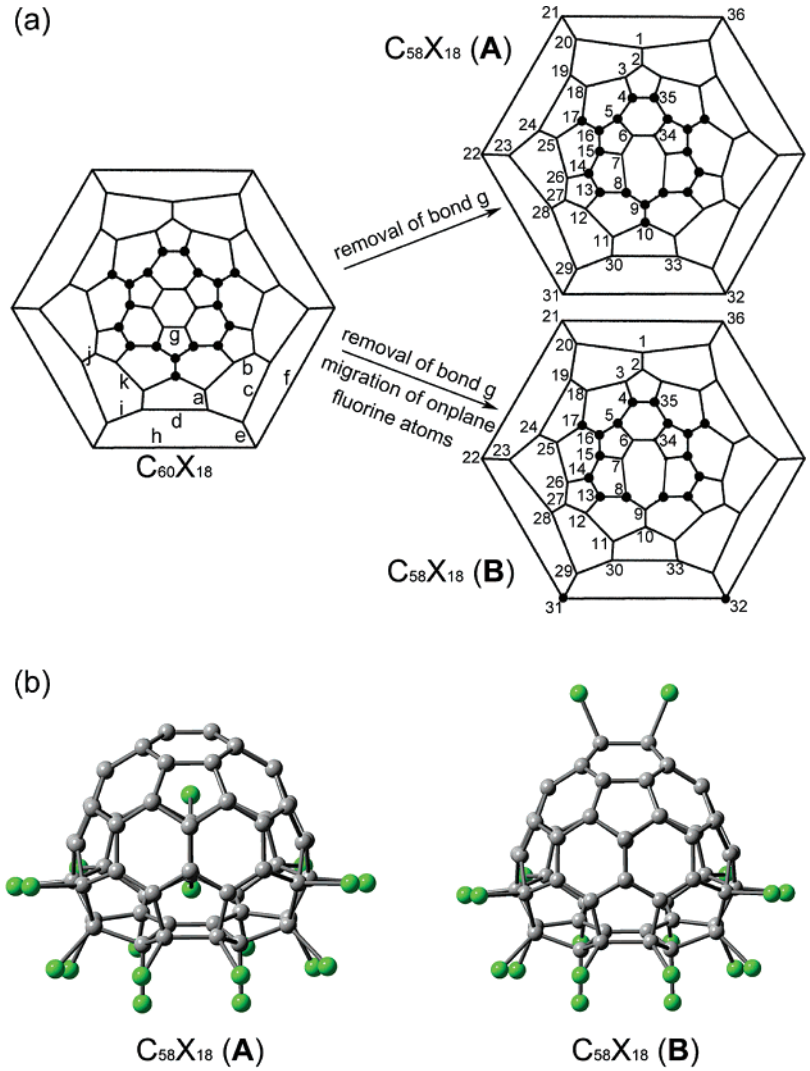

Figure 1. (a) Schlegel diagrams for C_{3v}-$C_{60}X_{18}$, C_s-$C_{58}X_{18}$ (**A**), and C_s-$C_{58}X_{18}$ (**B**) showing the notations of the bonds (a−k) and Arabia numerals (1−35); ● = X (X = H, F, and Cl). Note that F (9) and F (10) atoms in structure **A** are on-plane fluorine atoms. (b) The B3LYP/6-31G(d,p) optimized structures $C_{58}X_{18}$ (**A**) and $C_{58}X_{18}$ (**B**).

hyperpolarizabilities of these derivatives are predicted with the ZINDO[25] method and sum-over-states (SOS)[26] model.

III. Results and Discussions

A. Geometries of $C_{58}X_{18}$. There are seven ways to remove a 6:5 C−C bond (see Figure 1a) and four ways to remove a 6:6 C−C bond (see Figure 1a) from $C_{60}X_{18}$ fullerene derivatives (X = H, F, and Cl). Optimization of these eleven different $C_{58}X_{18}$ geometries along with the characterized structure[18] is performed at B3LYP/3-21G level. Among these 12 different structures, there are two isomers obtained by removal of bond *g* (see Figure 1a) from $C_{60}X_{18}$, one is labeled as structure **A** and the other one is labeled as structure **B,** as shown in Figure 1a. It should be mentioned that the structure **B** is produced not only by removal of bond *g* but also with the migration of the onplane fluorine pair. The structure of $C_{58}F_{18}$ (**B**) has been characterized by mass spectrometry and fluorine nuclear magnetic resonance spectroscopy. As shown in Table 1, the structure **A** is the most stable isomer among the 12 different structures of $C_{58}H_{18}$ and $C_{58}F_{18}$, followed by the structure **B**, which is just 6.91 and 12.29 kcal/mol higher in energy for $C_{58}H_{18}$ and $C_{58}F_{18}$, respectively. The relative energies of other structures are at least larger than 36.87 and 35.14 kcal/mol for $C_{58}H_{18}$ and $C_{58}F_{18}$, respectively. It is necessary to mention that another stable compound $C_{58}F_{17}CF_3$ (**B**) observed experimentally[18] possesses similar structure to $C_{58}F_{18}$ (**B**), except that the CF_3 group substitutes for F atom (8, see Figure 1). The calculations show that $C_{58}F_{17}CF_3$ (**A**) possesses lower energy than $C_{58}F_{17}CF_3$ (**B**) by 11.83 kcal/mol (at B3LYP/3-21 g level), of which the relative energy is close to that (12.29 kcal/mol) of $C_{58}F_{18}$ (**B**). Note that the structures of $C_{58}F_{17}CF_3$ (**A**) and $C_{58}F_{17}$-

TABLE 1: Relative Energies (in kcal/mol) of the Different Isomers for $C_{58}X_{18}$ (X = H, F, and Cl) Based on BL3YP/3-21G Predictions[a]

removal bond	$C_{58}H_{18}$	$C_{58}F_{18}$	$C_{58}Cl_{18}$
a	36.87	35.14	21.73
b	53.44	55.63	50.30
c	48.33	47.94	40.95
d	80.45	79.49	69.66
e	51.74	51.57	41.97
f	56.06	55.88	50.15
g (**A**)	0.00	0.00	26.68
g (**B**)	6.91	12.29	0.00
h	103.17	103.96	94.48
i	81.64	80.00	75.53
j	74.13	72.13	57.84
k	69.09	63.71	60.66

[a] The notations for bonds (a−k) and structures (**A**, **B**) are presented in Figure 1.

TABLE 2: The Symmetries, Relative Energies, HOMO and LUMO Energies, HOMO−LUMO Gaps, NICS Values, Vertical Electron Affinities(VEA), and Vertical Ionization Potentials (VIP) for C_{58}, $C_{58}X_{18}$ (A), $C_{58}X_{18}$ (B), and $C_{60}F_{18}$[a]

isomer	symmetry	E_{rel}	E_{HOMO}	E_{LUMO}	E_g	NICS	VEA	VIP
C_{58}	C_s		−5.37	−3.82	1.55	−5.1	2.58	6.76
$C_{58}H_{18}$ (**A**)	C_s	0.00	−5.28	−1.87	3.41	−13.2	0.66	6.49
$C_{58}H_{18}$ (**B**)	C_s	8.41	−4.83	−1.70	3.13	−10.0	0.53	6.04
$C_{58}F_{18}$ (**A**)	C_s	0.00	−7.28	−3.83	3.45	−13.9	2.58	8.49
$C_{58}F_{18}$ (**B**)	C_s	9.36	−7.04	−4.20	2.84	−11.3	3.00	8.24
$C_{58}Cl_{18}$ (**A**)	C_s	0.00	−6.99	−3.83	3.16	−13.2	2.76	8.08
$C_{58}Cl_{18}$ (**B**)	C_s	−29.44	−6.74	−4.10	2.64	−10.4	3.06	7.79
$C_{60}F_{18}$	C_{3v}		−7.30	−3.68	3.62	−15.4	2.50	8.60

[a] The relative energies of $C_{58}X_{18}$ (**B**) are evaluated with respect to the energies of $C_{58}X_{18}$ (**A**). The relative energies are in kcal/mol, NICS in ppm, and the other values are in eV. All of the predictions are made at B3LYP/6-31G(d,p) level.

CF_3 (**B**) are shown in Figure S1 as Supporting Information. We suspect that the successful isolation of $C_{58}F_{18}$ (**B**) rather than $C_{58}F_{18}$ (**A**) is due to the particular condition in experiment. As to $C_{58}Cl_{18}$, however, $C_{58}Cl_{18}$ (**B**) is the most stable structure among the 12 different geometries, and $C_{58}Cl_{18}$ (**A**) is 26.68 kcal/mol less stable. Note that there is one $C_{58}Cl_{18}$ isomer, formed by removal of a bond from $C_{60}Cl_{18}$, possesses a close energy [with relative energy of 21.73 kcal/mol to $C_{58}Cl_{18}$ (**B**)] with that of $C_{58}Cl_{18}$ (**A**). In our study, we focus on the geometries and electronic properties of $C_{58}X_{18}$ (**A**) and $C_{58}X_{18}$ (**B**).

The geometries of $C_{58}X_{18}$ (**A**) and $C_{58}X_{18}$ (**B**) are further optimized with B3LYP/6-31G(d), and the structures are presented in Figure 1b. To confirm the accuracy of B3LYP/6-31G(d) method, we also optimize the structure of $C_{60}F_{18}$ and compare the bond lengths with experiment.[27] The calculations show that the C−C bond lengths are longer than the experimental values by 0.006 Å, and the C−F bond lengths are just shorter than the experimental values by 0.004 Å in average, suggesting the reliability of B3LYP/6-31G(d) method. The $C(sp^2)-C(sp^2)$, $C(sp^2)-C(sp^3)$, and $C(sp^3)-C(sp^3)$ bond lengths of $C_{58}X_{18}$ (**A**) and $C_{58}X_{18}$ (**B**) (X = H, F, and Cl) are listed in Table S1 (available in Supporting information), and the C−X bond lengths are shown in Table S2. From the comparison of the bond lengths presented in Table S1, it is clear that the geometries of C_{58} moieties of $C_{58}X_{18}$ (**A**) and $C_{58}X_{18}$ (**B**) (X = H, F, and Cl) are nearly the same, except for small deviation of the $C(sp^3)-C(sp^3)$ bonds. Take the $C_{58}H_{18}$ (**B**), $C_{58}F_{18}$ (**B**), and $C_{58}Cl_{18}$ (**B**) structures for example: the averaged $C(sp^3)-C(sp^3)$ bond lengths are 1.583, 1.589, and 1.620 Å, respectively, with difference less than 0.04 Å. However, these average $C(sp^3)-C(sp^3)$ bond lengths are significantly longer than the average C−C bond length (1.420 Å) at the same sites in pure C_{58}, of which the elongation of the C−C bonds are mainly caused by the hybridization of carbon atoms from sp^2 to sp^3. The C−X bond lengths (X = H, F, and Cl) at different sites in $C_{58}X_{18}$ fullerene derivatives are listed in Table S2, and the averaged C−H, C−F, and C−Cl bond lengths are 1.098, 1.378, and 1.823 Å, respectively. The average C−F bond length in our calculations agrees well with the C−F bond lengths in $C_{50}F_{10}$[28] and $C_{60}F_{18}$,[27] and the average C−Cl bond length in $C_{58}Cl_{18}$ agrees well with C−Cl bond lengths in compounds $C_{60}Cl_{28}$ and $C_{60}Cl_{30}$ reported recently.[29,30] The $C(sp^3)-C(sp^3)$ and C−X bond lengths in $C_{58}X_{18}$ (**A**) are presented in Table S1 and Table S2, respectively, and they are similar to those in $C_{58}X_{18}$ (**B**).

B. Aromatic Character of $C_{58}X_{18}$. Aromaticity is often discussed in terms of various criteria such as energetics, magnetics, and geometry. As a measure of aromaticity, NICS proposed by Schleyer et al.[21] is based on magnetic shieldings. NICS values are computed at selected points inside or around a molecule. For fullerenes, the computed NICS values at the center of fullerenes based on B3LYP/6-31G(d) agree well with the endohedral ^{3}He NMR chemical shifts measured,[31] and thus it is an effective way to evaluate aromaticity. According to the so-called NICS characterization, the aromaticity is characterized by a negative NICS value, antiaromaticity by a positive NICS, and nonaromaticity by a value close to zero.

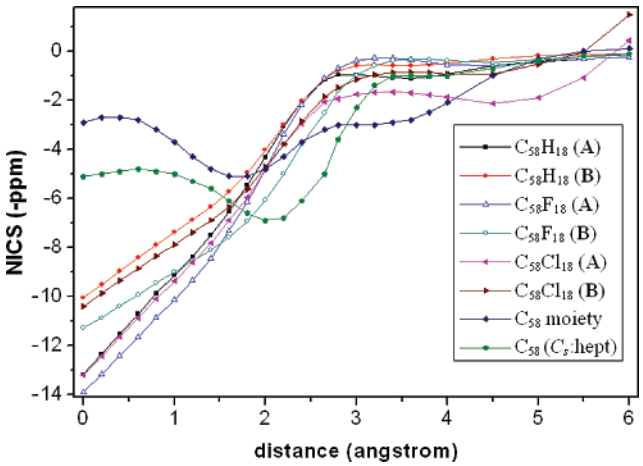

Figure 2. The NICS variation with distance from the cage center through the middle points of the heptagon in $C_{58}X_{18}$ (**A**), $C_{58}X_{18}$ (**B**), C_{58} moiety of $C_{58}F_{18}$ (**A**), and pure C_{58} (C_s:hept).

To get insight into the aromatic character of $C_{58}X_{18}$ (**A**) and $C_{58}X_{18}$ (**B**) (X = H, F, and Cl), the NICS values at the center of C_{58} moieties in $C_{58}X_{18}$ are calculated and compared to that of $C_{60}F_{18}$. All of the calculations are performed based on GIAO-B3LYP/6-31G(d,p) method. Based on our calculations, the NICS value of $C_{60}F_{18}$ cage is −15.4 ppm, and the values for $C_{58}X_{18}$ (both **A** and **B**) are slightly less negative, varying from −10.0 to −13.9 ppm as shown in Table 2. The $C_{58}X_{18}$ (**A**) structures possess more negative NICS values (from −13.2 to −13.9 ppm) than those (from −10.0 to −11.3 ppm) of $C_{58}X_{18}$ (**B**), both of which exhibit large aromatic character. Fluorofullerene $C_{58}F_{18}$ (**A**) not only has lower energy than the characterized $C_{58}F_{18}$ (**B**) but also possesses more negative NICS value of −13.9 ppm at the center of cage than −11.3 ppm of $C_{58}F_{18}$ (**B**), which suggests that $C_{58}F_{18}$ (**A**) is stable and can be isolated experimentally.

As we know, the aromatic ring in $C_{60}X_{18}$ is disrupted when the bond *g* is removed to form $C_{58}X_{18}$, which slightly affects the aromaticity of $C_{60}X_{18}$. How is the aromatic character of the heptagon in $C_{58}X_{18}$ (**A**) and $C_{58}X_{18}$ (**B**)? To clarify this question, we calculate the NICS values at different sites, moving from the cage center toward the heptagon (central point) in $C_{58}X_{18}$. As shown in Figure 2, for each $C_{58}X_{18}$, the NICS value becomes more positive gradually when NICS index (Bq atom) moves from the cage center toward the heptagon. The NICS values at the center of heptagon in $C_{58}H_{18}$ (**A**), $C_{58}F_{18}$ (**A**), $C_{58}Cl_{18}$ (**A**), $C_{58}H_{18}$ (**B**), $C_{58}F_{18}$ (**B**), and $C_{58}Cl_{18}$ (**B**) are −1.2, −1.1,

−1.9, −1.1, −2.5, and 1.5 ppm, respectively, exhibiting nearly nonaromatic character. These values are close to the NICS value of −2.5 ppm at the center of heptagon in pure C_{58} fullerene [labeled as C_{58} (C_s:hept)],[17] suggesting that the change of hybridization of some carbon atoms in the pentagon from sp^2 to sp^3 just slightly affects the aromatic character at the center of the heptagon (viz., the aromaticity of the heptagon is mainly σ aromaticity through the σ bonds contributions). In addition, we also calculated the NICS values from the cage center of C_{58} (C_s:hept) toward the central point of heptagon. Compared to $C_{58}X_{18}$, the NICS values of C_{58} (C_s:hept) near the cage center with distance less than 1.4 Å are less negative. The evolutional tendency of NICS values in C_{58} is similar to that of $C_{58}X_{18}$ when distance is larger than 2.0 Å, although the values are slightly different. This suggests that the addition of $9X_2$ changes the electronic structure of the C_{58} cage and thus affects the aromatic character of the cage center. Besides, the NICS values in the C_{58} moiety of $C_{58}F_{18}$ (**A**) is also calculated and presented in Figure 2. The structure of C_{58} moiety of $C_{58}F_{18}$ (**A**) is obtained through the elimination of $9F_2$ upon the optimized $C_{58}F_{18}$ (**A**). Compared to pure C_{58} (C_s:hept), the NICS values inside the cage of C_{58} moiety are slightly less negative, of which the difference should be caused by the distortion of the C_{58} cage within $C_{58}X_{18}$. In summary, the addition of $9X_2$ greatly changes the aromatic character of cage center and has slight affect to the center of heptagon. The large difference of NICSs at the center of the cages between C_{58} and $C_{58}X_{18}$ reveal that the relatively strong aromaticity of $C_{58}X_{18}$ is attributed to the addition of $9X_2$.

C. Electronic Properties of $C_{58}X_{18}$. To get insight into the electronic properties of the two different structures **A** and **B**, the energies of the highest occupied molecular orbital (E_{HOMO}) and the lowest unoccupied molecular orbital (E_{LUMO}), the HOMO−LUMO energy gap (E_g), vertical electron affinity (VEA), and vertical ionization potential (VIP) are evaluated at B3LYP/6-31G(d,p) level, as presented in Table 2. The E_{HOMO} for $C_{58}H_{18}$ (**A**) and $C_{58}H_{18}$ (**B**) are similar to that of C_{58}, while the E_{LUMO} is lifted by about 2 eV, thus resulting in the large energy gap E_g of 3.41 and 3.13 eV, respectively. However, the VEA values of $C_{58}H_{18}$ (**A**) and $C_{58}H_{18}$ (**B**) are 0.66 and 0.53 eV, respectively, much smaller than that of C_{58}, and the VIP values of $C_{58}H_{18}$ (**A**) and $C_{58}H_{18}$ (**B**) are slightly smaller than that of C_{58}, as shown in Table 2. As to the two different structures of $C_{58}F_{18}$ and $C_{58}Cl_{18}$, the electronic properties are different. The E_{HOMO} levels of $C_{58}F_{18}$ and $C_{58}Cl_{18}$ are significantly shifted down with respect to that of C_{58}, resulting in large HOMO−LUMO energy gaps, especially for $C_{58}F_{18}$ (**A**), of which the E_g is 3.45 eV, approaching that of C_{3v} $C_{60}F_{18}$ (3.62 eV). The calculated VIP of $C_{58}F_{18}$ and $C_{58}Cl_{18}$, from 7.79 to 8.49 eV, are larger than that of C_{58} by about 1.0 to 1.5 eV, and smaller than that (8.60 eV) of $C_{60}F_{18}$. In addition, the changes of E_{HOMO} and E_{LUMO} lead to the large VEA values of 3.00 and 3.06 eV for $C_{58}F_{18}$ (**B**) and $C_{58}Cl_{18}$ (**B**), respectively, larger than 2.58 eV of $C_{58}F_{18}$ (**A**), 2.76 eV of $C_{58}Cl_{18}$ (**A**), and 2.58 eV of C_{58}. Moreover, the VEA values of $C_{58}F_{18}$ (**B**) and $C_{58}Cl_{18}$ (**B**) are very close to that (3.04 eV) of the well-known D_{5h} $C_{50}Cl_{10}$[32] and about 0.5 eV higher than that of $C_{60}F_{18}$ (2.50 eV). It is known that halofullerenes, e.g., $C_{60}X_n$ (X = F and Cl), are good electron-acceptors with possible photonic/photovoltaic applications.[33] Like its $C_{60}X_n$ analogues, similar applications are expected for $C_{58}F_{18}$ and $C_{58}Cl_{18}$.

We also perform NBO analyses for $C_{58}X_{18}$ and present the natural atomic charges of C(sp^3) and X atoms in Table S2. The addition of X (X = H, F, and Cl) atoms to C_{58} changes the distribution of the natural atomic charges of atoms. From the analyses of natural atomic charges of atoms in $C_{58}X_{18}$, we can conclude that the addition of X atoms to the C_{58} mainly affects the charges of C(sp^3) atoms and the influence on other C(sp^2) atoms is negligible. For $C_{58}H_{18}$ (**A**) and $C_{58}H_{18}$ (**B**), the natural atomic charges of C(sp^3) and H atoms are from −0.22 to −0.29, 0.25 to 0.28, respectively. The redistribution of natural atomic charges in $C_{58}X_{18}$ brings about 2 electrons to C_{58} moiety of $C_{58}H_{18}$, which results in low values of VEA, 0.66 and 0.53 eV for $C_{58}H_{18}$ (**A**) and $C_{58}H_{18}$ (**B**), respectively. As to the two different structures of $C_{58}F_{18}$ ($C_{58}Cl_{18}$), the natural atomic charges of the C(sp^3) atoms are from 0.33 (−0.04) to 0.37 (−0.07), and natural atomic charges of F (Cl) atoms are from −0.33 (−0.01) to −0.35 (0.07), respectively, and they are significantly different from those of $C_{58}H_{18}$. It should be mentioned that the natural atomic charges of F atoms in $C_{58}F_{18}$ agree well with those in $C_{60}F_{18}$, in which the charges are from −0.33 to −0.35.

Binding 9 X_2 to C_{58} releases much of the strain of C_{58}, and the hydrogenation, fluorination, and chlorination reaction energies (eq 1−2; per H_2, F_2, and Cl_2) are −31.4, −113.7, −18.8, −30.5, −112.7, and −21.8 kcal/mol for $C_{58}H_{18}$ (**A**), $C_{58}F_{18}$ (**A**), $C_{58}Cl_{18}$ (**A**), $C_{58}H_{18}$ (**B**), $C_{58}F_{18}$ (**B**), and $C_{58}Cl_{18}$ (**B**), respectively. Compared to the hydrogenation, fluorination, and chlorination reaction energies (per H_2, F_2, and Cl_2) of D_{5h} $C_{50}X_{10}$ (−50.9, −131.8, −50.6 kcal/mol per H_2, F_2, and Cl_2 for $C_{50}H_{10}$, $C_{50}F_{10}$, and $C_{50}Cl_{10}$, respectively),[28,32] the reaction energies for $C_{58}X_{18}$ are smaller. This is not surprising since all of the 10 atoms are added to the sites of fused pentagons in C_{50} and greatly releases the strain of C_{50}, while only a few of the X atoms are added to the sites of fused pentagons in $C_{58}X_{18}$. In fact, as to $C_{58}X_{18}$, the addition of 9 X_2 also releases much of the strain in C_{58}, especially for $C_{58}F_{18}$, the fluorination reactions are highly exothermic, even larger than that (eq 3; 107.6 kcal/mol per F_2) of $C_{60}F_{18}$. As a result, although the removal of the bond *g* disrupts the aromatic ring of $C_{60}F_{18}$, the experimentally characterized $C_{58}F_{18}$ (**B**) structure, as well as $C_{58}F_{18}$ (**A**) structure, is much less strained. Consequently, the analyses of the reaction energies further confirm the large stabilities of $C_{58}X_{18}$ (**A**) and $C_{58}X_{18}$ (**B**):

$$C_{58} + 9X_2 \rightarrow C_{58}X_{18}\,(\mathbf{A}) \quad (1)$$

$$C_{58} + 9X_2 \rightarrow C_{58}X_{18}\,(\mathbf{B}) \quad (2)$$

$$C_{60} + 9F_2 \rightarrow C_{60}F_{18} \quad (3)$$

D. Infrared Spectra. Our goal is to provide hints that may be helpful for experimental identification of fullerenes. In particular, it will be useful to investigate if the IR spectra of different isomers are sufficiently different to allow for an unambiguous identification of each isomer. For this purpose, we investigate the IR spectra at the B3LYP/3-21G level, and focus on the main differences in the spectra of the two different structures $C_{58}X_{18}$ (**A**) and $C_{58}X_{18}$ (**B**), where X = H, F, and Cl.

As can be seen in Figure 3, all spectra have three regions: the first one (from 200 to 800 cm^{-1}) corresponds to cage breathing modes, the second one (from 950 to 1600 cm^{-1}) corresponds to the C−C stretching modes, and the third one corresponds to the C−X stretching modes. The cage breathing modes and the C−C stretching modes in $C_{58}X_{18}$ are related to the vibrational modes in heptagonal C_{58} which were studied in our previous work,[17] although their intensities vary as the addition of eighteen X atoms. The intensity of C−X stretching modes is significantly stronger than those of the first and the

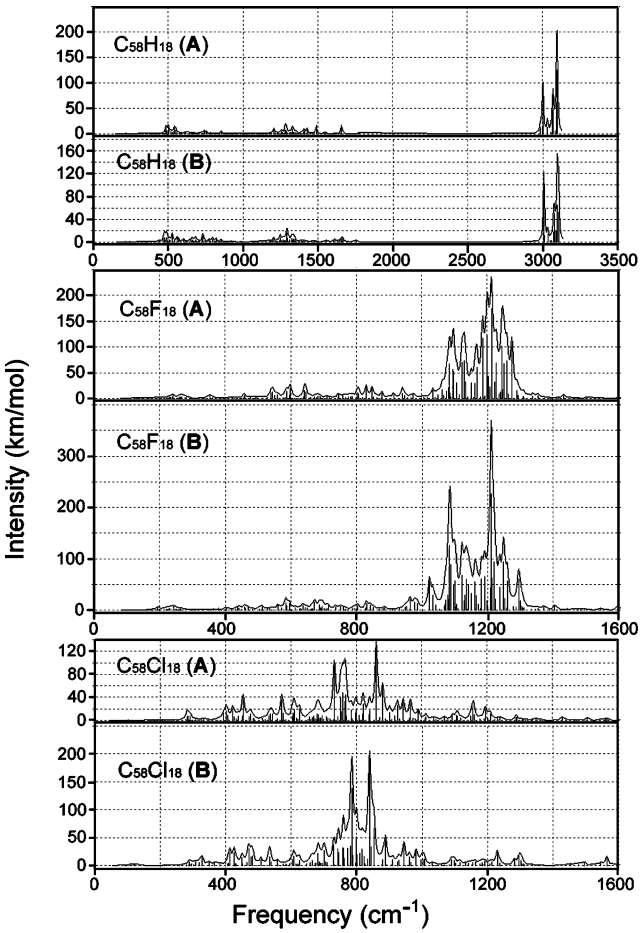

Figure 3. Simulated IR spectra for $C_{58}X_{18}$ (**A**) and $C_{58}X_{18}$ (**B**).

second regions of vibrational mode. As shown in Figure 3, the major regions of C−H, C−F, and C−Cl stretching modes are located in 3000−3110, 1050−1260, and 700−900 cm^{-1}, respectively. As to $C_{58}F_{18}$ (**A**) and $C_{58}F_{18}$ (**B**), there are three major characters: (a) The $C_{58}F_{18}$ (**B**) possesses the most intense peak of 226.8 km/mol at 1211 cm^{-1}, while the highest peak of $C_{58}F_{18}$ (**A**) is 174.3 km/mol at 1213 cm^{-1}, both of which correspond to the stretching modes of C(4)-F (see notation in Figure 1a) and C(16)-F bonds. (b) The peak at 1084 cm^{-1} (with intensity of 125.7 km/mol) of $C_{58}F_{18}$ (**B**) mainly corresponds to the stretching mode of C(31)-F bonds, while the intensity of the stretching of the in-plane C(9 and10)-F bonds in $C_{58}F_{18}$ (**A**) is less intense. (c) There are two intense peaks related to the stretching modes of C−C bonds in $C_{58}F_{18}$ (**B**) at 1023 and 1294 cm^{-1}, as shown in Figure 3, and $C_{58}F_{18}$ (**A**) has one intense peak related to stretching mode of C−C bonds at 1276 cm^{-1}. For $C_{58}Cl_{18}$ (**B**), the two most intense peaks locate at 786 and 840 cm^{-1}, of which the intensities are 138.7 and 170.4 km/mol, respectively. However, $C_{58}Cl_{18}$ (**A**) possesses less intense peaks with respect to those of $C_{58}Cl_{18}$ (**B**). The stretching modes of C−H bonds in $C_{58}H_{18}$ (**A**) and $C_{58}H_{18}$ (**B**) are similar, locate between 3000 and 3110 cm^{-1}. In summary, the two structures **A** and **B** show spectra that are qualitatively different when X = F and Cl, which may be helpful for future experimental characterization.

E. Electronic Spectra and Nonlinear Optical Properties of $C_{58}X_{18}$. The electronic spectra reflects the electronic structure of a system and it helps to identify the structure of the system. The system with large second-order hyperpolarizabilities may be served as promising NLO materials, and the system with extremely small second-order hyperpolarizabilities should help to search materials as optical protective materials. In our previous work, we have studied the NLO properties of fullerene C_{58} (C_s:hept) with one heptagon.[17] How will the addition of $9X_2$ to C_{58} (C_s:hept) affect the NLO properties (X = H, F, and Cl)? To clarify the problem, ZINDO/SOS is utilized to predict the static and frequency-dependent second-order hyperpolarizabilities for the $C_{58}X_{18}$ (**A**) and $C_{58}X_{18}$ (**B**).

Three different external field frequencies ω (ω = 0.6491, 1.1653, and 2.3305) are adopted to evaluate the second-order hyperpolarizability of $C_{58}X_{18}$ (**A**) and $C_{58}X_{18}$ (**B**), and the predicted values are listed in Table 3, as well as those of C_{58} (C_s:hept) from ref 17. Compared to those of C_{58} (C_s:hept), the static second-order hyperpolarizabilites of $C_{58}X_{18}$ (**A**) and $C_{58}X_{18}$ (**B**) are much smaller. For example, the static second-order hyperpolarizabilities of $C_{58}X_{18}$ (**A**) and $C_{58}X_{18}$ (**B**) are less than 6.0, greatly smaller than 15.34 of C_{58} (C_s:hept). Besides, the frequency-dependent second-order hyperpolarizaiblities are also much smaller than those of C_{58} (C_s:hept). For example, the intensity-dependent refractive index (IDRI) [$\gamma(-\omega;\omega,\omega,-\omega)$ (with ω = 1.1653 eV)] of $C_{58}X_{18}$ (**A**) and $C_{58}X_{18}$ (**B**) are less than 7.1, i.e., about 7.1% of that of C_{58} (C_s:hept). These results suggest that the addition of $9X_2$ greatly decreases the second-order hyperpolarizabilities, i.e., the ability of depolarization of $C_{58}X_{18}$ (**A**) and $C_{58}X_{18}$ (**B**) evidently increases. Why this happens? To get an insight into the second-order hyperpolarizabilities of $C_{58}X_{18}$ (**A**) and $C_{58}X_{18}$ (**B**), we analyze the evolution of the average static second-order hyperpolarizability γ, $\langle\gamma\rangle$, with the UV−vis spectra.

As shown in Figure 4, there are some common features as well as some different features for $C_{58}X_{18}$ (**A** and **B**) where X = H, F, and Cl. The common features are (1) with the addition of $9X_2$, not only the static second-order hyperpolarizabilities but also the oscillator strength of the excitations are evidently weaker than those of C_{58} (C_s:hept); (2) there are two strong broad absorption bands (4.0−6.5 and 8.0−10.5 eV) in the electronic spectra of C_{58} (C_s:hept), which contribute 74.0% to the static γ. However, the peaks in these two bands are evidently dispersed with the addition of $9X_2$ and their NLO contributions

TABLE 3: The Calculated Isotropically Averaged Values of the Second-Order Hyperpolarizability $\langle\gamma\rangle$ of C_{58} (C_s:hept), $C_{58}X_{18}$ (A), and $C_{58}X_{18}$ (B) Using ZINDO/SCI with the SOS Model (Units: 10^{-34} ESU) in the Presence of External Field ω[a]

	$\gamma(-3\omega;\omega,\omega,\omega)$			$\gamma(-2\omega;\omega,\omega,0)$			$\gamma(-\omega;\omega,\omega,-\omega)$		$\gamma(0;-\omega,\omega,0)$	
ω (eV)	0.0	0.6491	1.1653	0.6491	1.1653	0.6491	1.1653	2.3305	0.6491	1.1653
C_{58} (C_s:hept)	15.34	15.33	23.25	4.27	22.86	17.38	100.6	183.5	16.30	38.09
$C_{58}H_{18}$ (**A**)	5.5	6.7	6.6	6.1	7.7	5.9	6.6	18.6	5.7	6.1
$C_{58}H_{18}$ (**B**)	5.7	7.4	13.9	6.4	9.2	6.1	7.1	38.2	5.9	6.5
$C_{58}F_{18}$ (**A**)	4.4	5.2	3.2	4.8	5.7	4.7	5.1	33.4	4.6	4.8
$C_{58}F_{18}$ (**B**)	4.8	6.0	17.0	5.3	6.9	5.1	5.7	23.6	5.0	5.4
$C_{58}Cl_{18}$ (**A**)	5.3	6.3	5.2	5.7	7.0	5.6	6.1	18.2	5.4	5.8
$C_{58}Cl_{18}$ (**B**)	5.8	7.3	10.6	6.4	8.6	6.2	6.9	36.6	6.0	6.5

[a] The values for C_{58} (C_s:hept) are from ref 17.

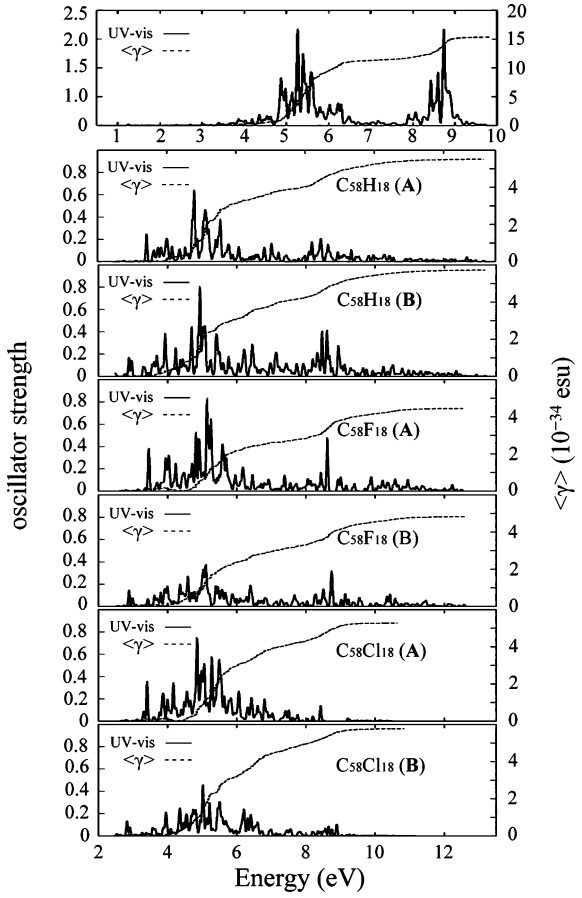

Figure 4. The electronic spectra of $C_{58}X_{18}$ (**A**) and $C_{58}X_{18}$ (**B**), as well as C_{58} (C_s:hept) predicted by ZINDO/SCI and the static second-order hyperpolarizability $\langle\gamma\rangle$ obtained by ZINDO/SOS. The UV−vis plot is broadened by 0.05 eV.

greatly decrease compared to those in C_{58} (C_s:hept), which directly results in the small static γ values of $C_{58}X_{18}$. The different features are listed below: (1) among the $C_{58}X_{18}$ (X = H, F, and Cl) derivatives, the static γ of fluorofullerene $C_{58}F_{18}$ with both **A** and **B** structures are the smallest, which suggest that the fluorofullerene may be good candidate of material as optical protective materials. (2) for $C_{58}H_{18}$ and $C_{58}F_{18}$, there are some weak peaks when the energy of electron excitation is larger than 10 eV, but the contribution of electron excitations from 10.0 to 12.0 is nearly zero for $C_{58}Cl_{18}$; (3) the electronic spectra of structure **B** is different from that of structure **A**. For example, the first evident peak of $C_{58}X_{18}$ (**B**) appears at about 2.9 eV, whereas the first evident peak of $C_{58}X_{18}$ (**A**) appears at about 3.4 eV, which may help to identify the different isomers. In summary, the addition of $9X_2$ greatly affects the electronic structures of C_{58} (C_s:hept) and the second-order hyperpolarizabilities are greatly decreased. Both the static and frequency-dependent second-order hyperpolarizabilities of $C_{58}X_{18}$ are extremely small, which may enable them as optical protective material.

IV. Conclusions

Systematic predictions have been performed on the stabilities and electronic properties of heptagonal $C_{58}X_{18}$ (**A**) and $C_{58}X_{18}$ (**B**), where X = H, F, and Cl. The $C_{58}F_{18}$ (**A**) isomer is found to be 9.36 kcal/mol more stable than the experimentally characterized $C_{58}F_{18}$ (**B**), and $C_{58}H_{18}$ (**A**) is 8.41 kcal/mol more stable than $C_{58}H_{18}$ (**B**), while $C_{58}Cl_{18}$ (**B**) is 29.44 kcal/mol lower in energy than $C_{58}Cl_{18}$ (**A**). The analyses of NICS values at the cage center show that $C_{58}X_{18}$ (**A**) possess larger values (−13.2 to −13.9 ppm) than those (−10.0 to −11.3 ppm) of $C_{58}X_{18}$ (**B**), all of which exhibit aromatic character. Further investigations show that the hydrogenation, fluorination, and chlorination reaction energies of $C_{58}X_{18}$ release much of the strain of C_{58} fullerene, resulting in the large stabilities of $C_{58}X_{18}$. Especially, the fluorination reaction energies of $C_{58}F_{18}$ (−113.7 kcal/mol per F_2 for the structure **A** and −112.7 kcal/mol for the structure **B**) are highly exothermic, even larger than that (−107.6 kcal/mol per F_2) of $C_{60}F_{18}$, although the removal of the bond *g* disrupts the aromatic ring in $C_{60}F_{18}$. In addition, the NICS values at the center of heptagon in $C_{58}X_{18}$ fullerene derivatives are close to zero, suggesting the nonaromatic character of the heptagon. Since $C_{58}F_{18}$ (**B**) has been synthesized, $C_{58}F_{18}$ (**A**) with lower energy and larger NICS value should also be isolated experimentally. We speculate that the successful isolation of $C_{58}F_{18}$ (**B**) rather than $C_{58}F_{18}$ (**A**) may be due to the particular condition in experiment.

The large HOMO−LUMO gaps of $C_{58}X_{18}$ (**A**) and $C_{58}X_{18}$ (**B**) (X = H, F, and Cl), between 2.64 and 3.45 eV, along with their aromatic character reveal that they are stable fullerene derivatives. Different from $C_{58}H_{18}$, the addition of 9 X_2 (X = F and Cl) to C_{58} fullerene enhances the VEA values of $C_{58}F_{18}$ (**B**) and $C_{58}Cl_{18}$ (**B**), with even larger values than that of $C_{60}F_{18}$. Like its $C_{60}X_n$ analogues (X = F and Cl), which are good electron-acceptors with possible photonic/photovoltaic applications, similar applications are expected for $C_{58}F_{18}$ and $C_{58}Cl_{18}$. Simulated IR spectra for $C_{58}X_{18}$ (**A**) and $C_{58}X_{18}$ (**B**) show differences in positions and intensities of the corresponding bands (when X = F and Cl), which may be helpful for experimental identification of these derivatives. The analyses of the static and frequency-dependent second-order hyperpolarizabilities of $C_{58}X_{18}$ show that both the static γ values and the γ values at external field are much smaller than those of pure C_{58} (C_s:hept), *i.e.*, the depolarization upon addition of $9X_2$ is large. The static γ of fluorofullerene $C_{58}F_{18}$ is the smallest among $C_{58}X_{18}$ (X = H, F, and Cl), which suggest that fluorofullerene may be candidate as optical protective material, worthy of further investigations.

Acknowledgment. W.Q.T. thanks the startup fund from Jilin University. This work is also supported by Chinese Natural Science Foundation under Grant No. 20473031.

Supporting Information Available: C−C bond lengths, $C(sp^3)$−X bond lengths, and natural atomic charges of $C(sp^3)$ and X within $C_{58}X_{18}$ (**A**) and $C_{58}X_{18}$ (**B**). This material is available free of charge via the Internet at http://pubs.acs.org.

References and Notes

(1) Dresselhaus, M. S.; Dresselhaus, G.; Eklund, P. *Science of Fullerenes and Carbon Nanotubes*; Academic: New York, 1996.

(2) Holczer, K.; Klein, O.; Huang, S. M.; Kaner, R. B.; Fu, K. J.; Whetten, R. L.; Diederich, F. *Science* **1991**, *252*, 1154.

(3) Pekker, S.; Janossy, A.; Mihaly, L.; Chauvet, O.; Carrard, M.; Forro, L. *Science* **1994**, *265*, 1077.

(4) Dinnebier, R. E.; Gaunnarsson, O.; Brumm, H.; Koch, E.; Stephens, P. W.; Huq, A.; Jansen, M. *Science* **2002**, *296*, 109.

(5) Mickelson, W.; Aloni, S.; Han, W. Q.; Cumings, J.; Zettl, A. *Science* **2003**, *300*, 467.

(6) Kroto, H. W. *Nature (London)* **1987**, *329*, 529.

(7) Schmalz, T. G.; Seitz, W. A.; Klein, D. J.; Hite, G. E. *J. Am. Chem. Soc.* **1988**, *110*, 1113.

(8) Xie, S.; Gao, F.; Lu, X.; Huang, R.; Wang, C.; Zheng, X.; Liu, M.; Deng, S.; Zheng, L. *Science* **2004**, *304*, 699.

(9) Taylor, R. *Interdiscip. Sci. Rev.* **1992**, *17*, 161.

(10) Albertazzi, E.; Domene, C.; Fowler, P. W.; Heine, T.; Seifert, G.; Alsenoy, C. V.; Zerbetto, F. *Phys. Chem. Chem. Phys.* **1999**, *1*, 2913.
(11) Ayuela, A.; Fowler, P. W.; Mitchell, D.; Schmidt, R.; Seifert, G.; Zerbetto, F. *J. Phys. Chem.* **1996**, *100*, 15634.
(12) Díaz-Tendero, S.; Alcamí, M.; Martín, F. *J. Chem. Phys.* **2003**, *119*, 5545.
(13) Díaz-Tendero, S.; Alcamí, M.; Martín, F. *J. Chem. Phys.* **2005**, *123*, 184306.
(14) Hu, Y. H.; Ruckenstein, E. *J. Chem. Phys.* **2003**, *119*, 10073.
(15) Lee, S. U.; Han, Y.-K. *J. Chem. Phys.* **2004**, *121*, 3941.
(16) Ribas-Ariño, J.; Novoa, J. *J. Phys. Rev. B* **2006**, *73*, 035405.
(17) Chen, D.-L.; Tian, W. Q.; Feng, J.-K.; Sun, C.-C. *ChemPhysChem* [Online early access]. DOI: 10.1002/cphc.200600785.
(18) Troshin, P. A.; Avent, A. G.; Darwish, A. D.; Martsinovich, N.; Abdul-sada, A. K.; Street, J. M.; Taylor, R. *Science* **2005**, *309*, 278.
(19) Becke, A. *J. Chem. Phys.* **1993**, *98*, 5648.
(20) Frisch, M. J.; Trucks, G. W.; Schlegel, H. B.; Scuseria, G. E.; Robb, M. A.; Cheeseman, J. R.; Zakrzewski, V. G.; Montgomery, J. A., Jr.; Stratmann, R. E.; Burant, J. C.; Dapprich, S.; Millam, J. M.; Daniels, A. D.; Kudin, K. N.; Strain, M. C.; Farkas, O.; Tomasi, J.; Barone, V.; Cossi, M.; Cammi, R.; Mennucci, B.; Pomelli, C.; Adamo, C.; Clifford, S.; Ochterski, J.; Petersson, G. A.; Ayala, P. Y.; Cui, Q.; Morokuma, K.; Malick, D. K.; Rabuck, A. D.; Raghavachari, K.; Foresman, J. B.; ioslowski, J.; Ortiz, J. V.; Stefanov, B. B.; Liu, G.; Liashenko, A.; Piskorz, P.; Komaromi, I.; Gomperts, R.; Martin, R. L.; Fox, D. J.; Keith, T.; Al-Laham, M. A.; Peng, C. Y.; Nanayakkara, A.; Gonzalez, C.; Challacombe, M.; Gill, P. M. W.; Johnson, B. G.; Chen, W.; Wong, M. W.; Andres, J. L.; Head-Gordon,M.; Replogle, E. S.; Pople, J. A. *Gaussian 03*, revision C.02; Gaussian, Inc.: Wallingford CT, 2004.
(21) Schleyer, P. v. R.; Maerker, C.; Dransfeld, A.; Jiao H.; Hommes, N. J. R. v. E. *J. Am. Chem. Soc.* **1996**, *118*, 6317.
(22) Chen, Z.; Wannere, C. S.; Corminboeuf, C.; Puchta, R.; Schleyer, P. v. R. *Chem. Rev.* **2005**, *105*, 3842.
(23) Carpenter J. E.; Weinhold, F. *J. Mol. Struct. (THEOCHEM)* **1988**, *169*, 41.
(24) Reed, A. E.; Curtiss, L. A.; Weinhold, F. *Chem. Rev.* **1988**, *88*, 899.
(25) Ridley, J.; Zerner, M. C. *Theor. Chim. Acta* **1973**, *111*, 32.
(26) (a) Orr, B. J.; Ward, T. F. *Mol. Phys.* **1971**, *513*, 20. (b) Li, J.; Feng, J. K.; Sun, J. *Chem. Phys. Lett.* **1993**, *203*, 560.
(27) Neretin, I. S.; Lyssenko, K. A.; Antipin, M. Y.; Slovokhotov, Y. L.; Boltalina, O. V.; Troshin, P. A.; Lukonin, A. Y.; Sidorov, L. N.; Taylor, R. *Angew. Chem., Int. Ed.* **2000**, *39*, 3273.
(28) Chang, Y. F.; Zhang, J. P.; Hong, B.; Sun, H.; An, Z.; Wang, R. S. *J. Chem. Phys.* **2005**, *123*, 094305.
(29) Troshin, P. A.; Lyubovskaya, R. N.; Ioffe, I. N.; Shustova, N. B.; Kemnitz, E.; Troyanov, S. I. *Angew. Chem., Int. Ed.* **2005**, *44*, 234.
(30) Troyanov, S. I.; Shustova, N. B.; Popov, A. A.; Sidorov, L. N.; Kemnitz, E. *Angew. Chem., Int. Ed.* **2005**, *44*, 432.
(31) Chen, Z.; King, R. B. *Chem. Rev.* **2005**, *105*, 3613.
(32) Lu, X.; Chen, Z.; Thiel, W.; Schleyer, P. v. R.; Huang, R.; Zheng, L. *J. Am. Chem. Soc.* **2004**, *126*, 14871.
(33) Guldi, D. M. *Chem. Commun. (Cambridge)* **2000**, *321*.